THE JOURNAL OF BIOLOGICAL CHEMISTRY
Vol. 276, No. 22, Issue of June 1, pp. 18819–18827, 2001

Printed in U.S.A.

Mutations Leading to X-linked Hypohidrotic Ectodermal Dysplasia Affect Three Major Functional Domains in the Tumor Necrosis Factor Family Member Ectodysplasin-A*

Received for publication, February 9, 2001
Published, JBC Papers in Press, March 14, 2001, DOI 10.1074/jbc.M101280200

Pascal Schneider‡§, Summer L. Street¶, Olivier Gaide‡, Sylvie Hertig‡, Aubry Tardivel‡, Jürg Tschopp‡, Laura Runkel‖, Konstantinos Alevizopoulos, Betsy M. Ferguson¶, and Jonathan Zonana¶**

*From the ‡Institute of Biochemistry, BIL Biomedical Research Center, University of Lausanne, Boveresses 156, CH-1066 Epalinges, Switzerland, the ‖Department of Inflammation, Biogen Inc., Cambridge, Massachusetts 02142, **ApoTech Biochemicals, Croisettes 22, CH-1066 Epalinges, Switzerland, and the ¶Department of Molecular and Medical Genetics, Oregon Health Sciences University, Portland, Oregon 97201*

Mutations in the epithelial morphogen ectodysplasin-A (EDA), a member of the tumor necrosis factor (TNF) family, are responsible for the human disorder X-linked hypohidrotic ectodermal dysplasia (XLHED) characterized by impaired development of hair, eccrine sweat glands, and teeth. EDA-A1 and EDA-A2 are two splice variants of EDA, which bind distinct EDA-A1 and X-linked EDA-A2 receptors. We identified a series of novel EDA mutations in families with XLHED, allowing the identification of the following three functionally important regions in EDA: a C-terminal TNF homology domain, a collagen domain, and a furin protease recognition sequence. Mutations in the TNF homology domain impair binding of both splice variants to their receptors. Mutations in the collagen domain can inhibit multimerization of the TNF homology region, whereas those in the consensus furin recognition sequence prevent proteolytic cleavage of EDA. Finally, a mutation affecting an intron splice donor site is predicted to eliminate specifically the EDA-A1 but not the EDA-A2 splice variant. Thus a proteolytically processed, oligomeric form of EDA-A1 is required *in vivo* for proper morphogenesis.

The *ED1* gene encodes a protein, ectodysplasin-A (EDA),[1] recently recognized to be a member of the tumor necrosis factor (TNF) superfamily of ligands. Mutations within the *ED1* gene cause an X-linked recessive disorder, hypohidrotic or anhidrotic ectodermal dysplasia (ED1, XLHED) (Mendelian inheritance in man 305100), involving abnormal morphogenesis of teeth, hair, and eccrine sweat glands. Various splice forms of the ED1 transcript have been detected, but two isoforms differing only by two amino acids, EDA-A1 (391 aa) and EDA-A2 (389 aa), contain a TNF homology domain (1–3). EDA is a type II transmembrane protein with a small N-terminal intracellular domain and a larger C-terminal extracellular domain containing a $(Gly\text{-}X\text{-}Y)_{19}$ collagen-like repeat with a single interruption and a C-terminal TNF homology domain (Fig. 1*A*). The TNF homology domain is similar to other members of the TNF family, consisting of 10 predicted anti-parallel β-sheets linked by variable loops (Fig. 1*A*). TNF family ligands homotrimerize to form a pear-shaped quaternary structure able to bind a receptor molecule at each monomer-monomer interface (4, 5). The closest EDA homologues in the TNF family are BAFF/BLyS, APRIL, and TWEAK, although none of them contains collagen-like repeats (6–9). All four ligands contain consensus sequences for proteolytic cleavage by furin within their extracellular domain. In the case of EDA, two overlapping consensus sites are located between the transmembrane and the collagen-like domains (Fig. 1*A*). EDA-A1, but not EDA-A2, has been shown to specifically bind to EDAR, a member of the TNF receptor superfamily that, like most members of the TNF receptor family, activates the NF-κB and c-Jun N-terminal kinase pathways (3, 10). Mutations in DL (EDAR), the human homologue of the murine downless locus, produce an identical phenotype to loss of function of EDA (11, 12). XEDAR, another member of the TNF receptor superfamily that also activates the NF-κB pathway, binds EDA-A2 but not EDA-A1. Although EDA-A1 and EDA-A2 are closely related splice variants, the respective proteins appear to have different patterns of expression in mouse skin and hair follicles (3). Intracellular signals elicited by EDA *in vivo* rely at least in part on the activation of NF-κB, because a rare form of HED associated with immunodeficiency (HED-ID) correlates with mutations in NEMO/IKK-γ, an essential component of the NF-κB pathway (13).

In order to get insight into the structure-function relationship of EDA, we identified 44 mutations (17 of which have not been reported previously) in unrelated families with XLHED and studied their effect on the properties of EDA *in vitro*. The mutations clustered in three functionally important domains as follows: a TNF homology domain necessary for receptor binding, a bundle-forming collagen domain, and a cleavage site for a furin protease. This indicates that the receptor binding ability of EDA and also its oligomerization and proteolytic processing to a soluble form are critical events for its action *in vivo*.

* This work was supported in part by grants from the Swiss National Science Foundation (to P. S. and J. T.), National Institutes of Health Grant DE11311 (to B. F. and J. Z.), and by the National Foundation for Ectodermal Dysplasias (to J. Z.). The costs of publication of this article were defrayed in part by the payment of page charges. This article must therefore be hereby marked "*advertisement*" in accordance with 18 U.S.C. Section 1734 solely to indicate this fact.

§ To whom correspondence should be addressed: Institute of Biochemistry, University of Lausanne, Ch. des Boveresses 155, CH-1066 Epalinges, Switzerland. Tel.: 41 21 692 5709; Fax: 41 21 692 5705; E-mail: pascal.schneider@ib.unil.ch.

[1] The abbreviations used are: EDA, ectodysplasin-A; TNF, tumor necrosis factor; XLHED, X-linked hypohidrotic ectodermal dysplasia; EDAR, ectodysplasin-A1 receptor; XEDAR, X-linked ectodysplasin-A2 receptor; FasL, Fas ligand; aa, amino acids; SSCP, single-stranded conformation polymorphism; CHO, Chinese hamster ovary; PCR, polymerase chain reaction; PBS, phosphate-buffered saline; wt, wild type; ELISA, enzyme-linked immunosorbent assay.

MATERIALS AND METHODS

Families Analyzed—Seventy apparently unrelated families with hypohidrotic ectodermal dysplasia were identified by clinicians at various centers and recruited into a research study approved by the institutional review board of the Oregon Health Sciences University. Consent was obtained for the use of clinical information, relevant family history, and DNA samples. Family histories and clinical data were provided by the clinical centers. A single individual was screened for mutations in each family. Fifty affected males had the classical findings of hypodontia, hypotrichosis and hyphidrosis (decreased amount of teeth, hair, and sweat glands, respectively), whereas 20 carrier females were either obligate carriers or had clear manifestations of the disorder. 38 of the families had more than one affected individual (multiplex families), whereas the remaining 32 cases were sporadic (simplex families). A subset of the families had been analyzed previously and shown to have no detectable mutations within exon 1 of ED1 (14).

Mutation Detection—The eight exons coding for EDA-A1 and EDA-A2 were amplified by PCR from genomic DNA of patients and controls using a Stratagene Robocycler with the primers and conditions listed in Table I. Genomic DNA samples from controls and 15 known mutations, previously detected by complete sequencing of the *ED1* gene, were run as controls under the same conditions utilizing single-stranded conformation polymorphism (SSCP) analysis (14). PCR fragments from exons 1, 5, and 9 were digested to produce restriction fragments in the 100–270-base pair range (Table I). All samples were then denatured at 95 °C for 5 min, chilled on ice, and electrophoresed on a 0.5× MDE™ polyacrylamide gel (FMC Corp.) at room temperature for SSCP analysis. Electrophoresis of all samples, except for those from exon 1, was performed in 10% glycerol. DNA was visualized by silver staining (14). Samples having abnormally migrating bands were re-amplified from stock genomic DNA, purified by use of Geneclean (Bio 101), and sequenced on both strands by use of ABI end-terminator chemistry on either a 373A or 377 automated sequencer. A previously identified recurrent mutation, $G^{467} \rightarrow A$ (R156H) was not detectable by SSCP using several sets of conditions. However, the mutation eliminates a restriction site for Fnu4H1 (gc/ngc). Therefore, PCR fragments from exon 3 with normally migrating bands on SSCP were digested with Fnu4H1 and electrophoresed on a 3% agarose gel. Genomic DNA from the mothers of individuals with confirmed mutations were also sequenced. Sequence alignments were performed using a pairwise sequence alignment program.

Production of Recombinant Proteins—Cloning of ligands and receptors in suitable vectors and expression of the recombinant proteins in 293T cells were performed essentially as described previously (15). The source of cDNAs used in this study was as follows: mouse EDA-A1 (aa 245–391) and EDA-A2 (aa 245–389) were amplified by nested reverse transcriptase-PCR from mouse lung and brain cDNAs, respectively (using primer pair 5′GGA TTC CAG GAA CAA CTG TTA TGG3′ and 5′CCT ACA CAC AGC AAG CAC CTT AGA G3′ for the initial PCR). In this region, the murine and human proteins are 100% identical. Full-length cDNAs for hEDA and hEDAR have been described earlier (2, 12), and XEDAR cDNA was from clone 5091511 (LifeSeq® Gold, Incyte Genomics, Palo Alto, CA). The expression construct for XEDAR:Fc carried a human immunoglobulin μ chain signal sequence, the region coding for amino acids 1–135 of XEDAR flanked by *Aat*II and *Sal*I sites, and the Fc portion of human IgG1, in a modified PCR-3 expression vector (Invitrogen). The extracellular domain of hEDAR (aa 1–183) was cloned into the Fc fusion expression vector. Expression vectors for various soluble forms of FLAG-tagged EDA were constructed in a vector containing the signal peptide of hemagglutinin (see Fig. 1*B*) as follows: EDA-A1 Glu^{245} (aa 245–391), EDA-A2 Glu^{245} (aa 245–389), EDA-A1 Ser^{160} (aa 160–391), and EDA-A1 Ser^{66} (aa 66–391). The following point mutations were generated by PCR-based methods in both EDA-A1 and EDA-A2 E245: H252L, Y343C (Y341C), A356D (A354D), S374R (S372R), T378M (T376M) (mutations in parentheses refer to EDA-A2 which lacks amino acids 307 and 308. For the sake of clarity, the EDA-A1 mutant nomenclature will be used for both ligands.). The following mutants were also constructed: EDA-A1 Ser^{66} R153C, EDA-A1 Ser^{66} R156C, and EDA-A1 Ser^{66} Δ185–196. For the expression vectors for EDA, FasL fusion proteins contained the hemagglutinin signal peptide, a FLAG tag, the entire or truncated collagen domain of EDA (aa Ser^{160}–Arg^{244}, aa Ser^{160}–Arg^{244} Δ185–196, aa Ser^{160}–Arg^{244} Δ218–223, aa Ser^{160}–Arg^{244} G207R, aa Gly^{210}–Arg^{244}), and the TNF homology domain of FasL (aa Glu^{139}–Leu^{281} of hFasL). Finally, mutations C86R and R87P were introduced in hEDAR:Fc. All constructs were sequenced on both strands. CHO cells were transfected with Polyfect reagent (Qiagen), according to the manufacturer's instructions.

Cell Lines—HEK-233T cells were maintained in Dulbecco's modified Eagle's medium and CHO $dhfr^-$ cells in α-minimum essential medium containing ribonucleosides and deoxyribonucleosides (Life Technologies, Inc.). Culture media were supplemented with 10% of heat-inactivated fetal calf serum and antibiotics.

Deglycosylation—Denatured samples of EDA were submitted to deglycosylation with peptide *N*-glycanase F for 16 h at 37 °C, following the manufacturer's recommendations (New England Biolabs).

Receptor Binding ELISA—The following steps were performed: (*a*) coating with 5 μg/ml mouse anti-human IgG antibodies (Jackson ImmunoResearch) in 50 mM carbonate buffer, pH 9.6; (*b*) incubation in block buffer (PBS, 0.5% Tween 20, 4% skimmed milk); (*c*) incubation with cell supernatants containing the indicated receptor:Fc fusion proteins (20 μl supernatant in 100 μl of incubation buffer: PBS, 0.05% Tween 20, 0.4% milk); (*d*) incubation with cell supernatants containing the indicated FLAG ligands (20 μl of supernatant in 100 μl of incubation buffer); (*e*) incubation with 0.5 μg/ml biotinylated anti-FLAG M2 antibody (Sigma) in incubation buffer; (*f*) incubation with horseradish peroxidase-coupled streptavidin (1/4000, Jackson ImmunoResearch) in incubation buffer. Alternatively, steps *d*—*f* were replaced by an incubation with horseradish peroxidase-coupled goat anti-human IgG. Four washing steps with PBS 0.05% Tween 20 were performed between incubations. 100 μl of *ortho*-phenylenediamine solution was added (Sigma fast *o*-phenylenediamine dihydrochloride tablet sets, Sigma), and the reaction was stopped by addition of 50 μl of 2 N HCl, and $A_{490\ nm}$ was taken.

Immunoprecipitations—FLAG ligands (about 100 ng in 100–400 μl of cell supernatants) were added to 5 μl of M2-agarose affinity matrix (Sigma). Receptors:Fc (about 500 ng in 100–400 μl of cell supernatants) were mixed with FLAG ligands (about 100 ng) and 5 μl of protein A-Sepharose. All samples were diluted to 1 ml with PBS and incubated on a rotating wheel for 1 h at 4 °C. Beads were recovered in mini-columns, washed with 2× 400 μl of PBS, and eluted in 15 μl of 0.1 M citrate/NaOH, pH 2.7. Neutralized eluates were prepared for Western blot analysis under reducing conditions. Membrane were probed with anti-FLAG M2 antibody or rabbit anti-EDA antibodies and subsequently reprobed with goat anti-human IgG antibodies.

Gel Permeation Chromatography—200 μl of transfected cell supernatants mixed with internal standards (40 μg of catalase and 100 μg of ovalbumin) was applied onto a Superdex-200 column and eluted in PBS at 0.5 ml/min. Fractions of 700 μl were collected and supplemented with 40 μg of lysozyme. Proteins were recovered by precipitation in chloroform/methanol and analyzed by Western blot.

Cytotoxic Assay—Cytotoxic assays in the presence or absence of 1 μg/ml of M2 antibody were performed as described previously, using the FasL-sensitive Jurkat cell line and measuring cell viability after 16 h with the phenazine methosulfate/3-[4, 5-dimethylthiazol-2-yl]-5-[3-carboxymethoxyphenyl]-2-[4-sulfonyl]-2*H*-tetrazolium test (16).

N-terminal Sequence Determination—EDA Ser^{66} and EDA Ser^{66} R153C were expressed in 293T cells. Supernatants (10 ml) were immunoprecipitated with 10 μg of EDAR:Fc and 20 μl of protein A-Sepharose as described above. Samples were reduced, blotted onto polyvinylidene difluoride membranes, and stained with Ponceau S. Bands of interest were submitted to automated Edman degradation using an ABI 120A gas phase sequencer coupled to an ABI 120A analyzer equipped with a phenylthiohydantoin C18 2.1 × 250 mm column. Data were analyzed using ABI 610 software.

Anti-EDA Antibodies—Anti-EDA rabbit anti-serum (AL166) was obtained by custom rabbit immunization using purified FLAG-EDA E245 as immunogen (Eurogentech, Seraing, Belgium). Serum was used at a dilution of 1/500 for Western blotting.

RESULTS

Identification of Mutations in HED—Twenty five different mutations of the *ED1* gene were detected in 44 of the 70 unrelated families analyzed (63%), and 9 were demonstrated to have occurred *de novo* (footnoted in Table II). As 17 of these mutations had not been described previously, the number of different *ED1* mutations identified to date in XLHED patients totals 53 (Table II). Analysis of the variants identified in this study showed a significantly non-random distribution of the mutations within the sequence of EDA. Fifteen separate families had mutations within the 7-amino acid domain (aa 153–159) encoding two adjacent potential furin cleavage sites. Mutations in 13 other families specifically affected the collagen-like domain. Ten of the families had 18 or 36 nucleotide

TABLE I
Primer pairs used for mutation detection in ED1

Exon	Forward primer (5′–3′)	Reverse primer (5′–3′)	Amplicon size	Restriction enzymes	Fragment size	Exon size	Annealing temperature
			bp			*bp*	*°C*
1	GTCGGCCGGGACCTCCTC	GCCGCCGCCCCTACTAGG	686	*Pst*I, *Taq*I	135, 147, 159, 245	396	66
3	ATGTTGGCTATGACTGAGTGG	CCCTACCAAGAAGGTAGTTC	248			106	57
4	GATCCCTCCTAGTGACTATC	CAGACAGACAATGCTGAAAGA	215			23	57
5	AAAAAAGTAACACTGAATCCTATT	CTCTCAGGATCACCCACTC	287	*Hin*fI	101, 146, 172	180	56
6	GGAAGTCAAAAGATTATGCCC	CTACCCAGGAAGAGAGCAAT	113			35	57
7	CTGAGCAAGCAGCCATTACT	GGGGAGAAGCTCCTCTTTG	156			52	57
8	ACTGAGTGACTGCCTTCTCT	GCACCGGATCTGCATTCTGG	214			131	57
9	TGTCAATTCACCACAGGGAG	CACAGCAGCACTTAGAGG	410	*Pst*I	141, 269	252	60

in-frame deletions eliminating 2 or 4 of the (Gly*XY*) repeats, and three families had missense mutations altering glycine residues. Nine missense mutations were detected within the TNF-like domain (aa 245–391), which is necessary and sufficient for receptor binding (3, 10). In the latter class of mutations, threonine 378 was altered in 4 independent families. In addition, 6 families had nonsense or frameshift mutations altering one or more of the domains cited above. Altogether, these data strongly suggest that the predicted furin, collagen, and TNF-like domains are essential for the function of EDA *in vivo*. Finally, a single splice site mutation was detected in the current study (IVS8 +5G → A), which affects the donor site of EDA-A1 but not that of EDA-A2. This mutation is predicted to eliminate EDA-A1 only, in contrast to all other mutations that alter both EDA-A1 and EDA-A2.

In an effort to understand the mechanism by which mutations detected in families with XLHED affect the function of EDA, we prepared a range of wild type and mutant recombinant EDA proteins and analyzed them in different *in vitro* assays. The mutations selected in this study are shown in bold in Table II, and the various protein constructs are schematized in Fig. 1*B*.

Binding Specificity of EDA-A1 and EDA-A2—We have previously shown the specific interaction of EDA-A1 with mouse EDAR (10), and we now document the interaction of EDA-A1 with human EDAR (Fig. 2, *A* and *C*). Recombinant EDA always migrated as a double band when analyzed by SDS-polyacrylamide gel electrophoresis, and both bands interacted with the receptor (Fig. 2*A*). Peptide *N*-glycanase F digestion of EDA-A1 indicated that the lower and upper bands corresponded to unglycosylated and *N*-glycosylated isoforms, respectively (Fig. 2*B*). To demonstrate the specificity of EDA/EDAR interaction, we expressed EDAR:Fc with mutations previously detected in two families with autosomal recessive hypohidrotic ectodermal dysplasia (online Mendelian inheritance in man 224900) (12). These point mutations either abolished (C87R) or strongly decreased (R89H) EDAR binding to EDA-A1. In addition, EDAR C87R was recovered in poor yield, suggesting folding or solubility defects (Fig. 2*A*). In agreement with recently published data (3), we found that the splice variant EDA-A2 interacted with a distinct receptor, XEDAR, and that XEDAR interacted only with EDA-A2 among 17 ligands of the TNF family tested (Fig. 2*C*).

Mutations in the TNF Homology Domain Affect Receptor Binding—Most of the selected EDA-A1 and EDA-A2 mutants affecting the TNF homology domain could be expressed as soluble, FLAG-tagged secreted proteins, but mutant A356D was entirely retained inside the cells, suggesting that it experienced folding or solubility problems (Fig. 3, *A* and *B*). Interestingly, the glycosylation pattern of the mutant S374R was indistinguishable from that of the wild type protein, although this mutation abolishes one of the two predicted *N*-glycosylation sites within the TNF-like domain (Fig. 2*B*). We deduce that *N*-glycosylation of EDA occurs on Asn^{313}, whereas Asn^{372} remains unglycosylated. All mutants lost their ability to interact with EDAR and XEDAR, in sharp contrast with the wild type proteins. The only exception was EDA-A1 S374R, which displayed weak and variable but apparently specific binding to EDAR (Fig. 3*A*). Surprisingly, only the unglycosylated isoform of this mutant interacted with the receptor.

In order to assess whether the mutations affected the quaternary structure of EDA, the size of the recombinant proteins was estimated by gel permeation chromatography (Fig. 4). Wild type EDA and the mutant Y343C eluted with an apparent mass of about 70-kDa, which is compatible with the predicted trimeric structure (Fig. 4). Mutants H252L and S374R displayed dissociation of the glycosylated and unglycosylated subunits, and the latter mutant had the propensity to elute as high molecular weight complexes. EDA-A1 T378M was poorly expressed and eluted apparently as high molecular weight aggregates, whereas EDA-A2 T378M was readily secreted and migrated with an apparent molecular weight smaller than that of the wild type protein. Taken together, the results indicate that, although the impact of the various mutations on the structure of EDA is different, they all affect interactions of EDA with both EDAR and XEDAR.

The Collagen Domain Induces Multimerization of EDA Trimers—Soluble, FLAG-tagged recombinant EDA with and without the collagen domain (EDA Ser^{160} and EDA Glu^{245}) and a deletion mutant lacking four of the Gly*XY* repeats (EDA Ser^{160} Δ185–196) all bound EDAR equally well (Fig. 5*A*). The collagen domain therefore appears not to play a direct role in receptor binding. In related proteins with collagen domains, such as C1q, collagen triple helices form a bundle, therefore assembling several globular trimeric heads into a single bouquet-like structure (17). In order to test whether the collagen region of EDA multimerizes, we generated EDA:FasL fusion proteins. We have shown previously that the TNF family member FasL is not cytotoxic as a soluble trimer, unless trimers are multimerized by means of cross-linking antibodies (here an anti-FLAG tag antibody) (16) (Fig. 5*C, upper left panel*). When FasL was fused to the collagen domain of EDA (amino acids Ser^{160}–Gly^{242}), its cytotoxic activity was increased by more than 100-fold, indicating that ligand multimerization had likely occurred. A similar effect was obtained with the collagen domain of EDA Δ185–196 and EDA Δ218–223, suggesting that these deletions did not affect multimerization. In contrast, no such aggregation effect was observed when the first half of the collagen domain was deleted (EDA Gly^{210}) or when the point mutation G207R was introduced (Fig. 5*C*).Taken together, these results indicate that the collagen triple helix of EDA forms multimers that are apparently not affected by in frame deletions but can be disrupted by point mutations.

Mutations in the Furin Cleavage Site Impair Proteolytic Processing at Arg^{159}—Mutation of Arg residues in the predicted furin cleavage sites is a common cause of XLHED, strongly suggesting that proteolytic processing of EDA at this site is necessary for its function *in vivo* (Table II). A soluble

TABLE II
EDA mutations in XLHED

Bold, selected for further studies.

Exon	Sequence variant	Mutation type	Protein change (codons)	No. this study	No. published	Total	Ref.
			Intracellular domain (1–40)				
1	46insC	FS	FS18		1	1	(25)
1	60–61ins8	FS	FS 20		1	1	(1)
1	121–122insC	FS	FS 41		1	1	(25)
1	$C^{67} \rightarrow T$	Nonsense	Q23X		1	1	(14)
			Transmembrane domain (41–63)				
1	$C^{160} \rightarrow T$	Missense	H54Y		1	1	(26)
1	$C^{164} \rightarrow G$	Missense	L55R		1	1	(27)
1	$T^{181} \rightarrow C$	Missense	Y61H		1	1	(25)
1	$C^{183} \rightarrow G$	Nonsense	Y61X		1	1	(28)
			Extracellular domain (64–391)				
1	$G^{187} \rightarrow A$	Missense	E63K		1	1	(14)
1	$G^{206} \rightarrow T$	Missense	R69L		2	2	(25)
1	252delT	FS	FS85		3	3	(25, 14)
1	$C^{382} \rightarrow T$	Nonsense	Q128X	1		1	
1	$C^{394} \rightarrow T$	Nonsense	Q132X		1	1	(25)
			Furin subdomain (150–159)				
3	$C^{457} \rightarrow T$	Missense	**R153C**	4		4	
3	$C^{463} \rightarrow T$	Missense	R155C	1	1	2	(2)
3	$C^{466} \rightarrow A$	Missense	R156S		1	1	(29)
3	$C^{466} \rightarrow T$	Missense	**R156C**	4	2	6	(1, 2)
3	$G^{467} \rightarrow A$	Missense	R156H	5[a]	1	6	(2)
3	$A^{474} \rightarrow T$	Missense	K158N	1		1	
			Collagen subdomain (180–235)				
5	546–581 del36	Deletion	In-frame 183–194del (Gly*XY*)×4	1		1	
5	553–588 del36	Deletion	**In-frame 185–196del** (Gly*XY*)**×4**	5[a]	2	7	(1, 2)
5	562–589 del28	Deletion	188–197del, FS198		1	1	(2)
5	$G^{566} \rightarrow A$	Missense	G189E	1		1	
5	572–589 del18	Deletion	In-frame 191–196del (Gly*XY*)×2	3[a]	1	4	(1)
5	595–613 del19	Deletion	199–204del, FS205	1		1	
5	599–600insC	FS	FS 201		1	1	(1)
5	$G^{619} \rightarrow A$	Missense	**G207R**	1		1	
5	$C^{626} \rightarrow T$	Missense	P209L		1	1	(2)
5	$G^{653} \rightarrow A$	Missense	G218D	1		1	
5	656–673 del18	Deletion	**In-frame 218–223del** (Gly*XY*) ×2	1		1	
5	659–676 del18	Deletion	In-frame 220–225del (Gly*XY*) ×2		1	1	(1)
5	663–697 del35	Deletion	221–233del, FS234	1[a]	1	2	(2)
5	$G^{671} \rightarrow C$	Missense	G224A		1	1	(2)
IVS5	A → G at 706–2	Splice	Altered splicing		1	1	(1)
6	$C^{730} \rightarrow T$	Nonsense	R244X	1[a]		1	
			TNF homology subdomain (250–391)				
7	$A^{755} \rightarrow T$	Missense	**H252L**		1	1	(2)
7	$C^{766} \rightarrow T$	Nonsense	Q256X	1		1	
8	$G^{822} \rightarrow A$	Nonsense	W274X	1		1	
8	$G^{871} \rightarrow T$	Missense	G291W		1	1	(1)
8	$G^{871} \rightarrow A$	Missense	G291R	2[a]	1	3	(1)
8	$G^{892} \rightarrow C$	Missense	D298H		1	1	(1)
8	$G^{895} \rightarrow A$	Missense	G299S	1	3	4	(1, 2)
IVS8	$G^{+5} \rightarrow A$	Splice	Altered splicing	1		1	
9	$A^{959} \rightarrow G$	Missense	Y320C	1		1	
9	$G^{961} \rightarrow T$	Nonsense	E321X		1	1	(2)
9	$A^{1028} \rightarrow G$	Missense	**Y343C**		1	1	(30)
9	$G^{1045} \rightarrow A$	Missense	A349T		2	2	(2)
9	$G^{1067} \rightarrow A$	Missense	**A356D**		1	1	(2)
9	$G^{1070} \rightarrow C$	Missense	R357P		1	1	(2)
9	$C^{1122} \rightarrow A$	Missense	**S374R**	1		1	
9	$A^{1132} \rightarrow C$	Missense	T378P	1		1	
9	$C^{1133} \rightarrow T$	Missense	**T378M**	3[a]		3	
			Totals	**44**	**42**	**86**	

[a] Mutations were demonstrated to have occurred *de novo.*

form of EDA containing the entire extracellular domain with a N-terminal FLAG tag (EDA Ser^{66}) was expressed in 293T cells. As expected, this protein was processed very efficiently, and a small 12-kDa N-terminal fragment bearing the FLAG tag was recovered in cell supernatants instead of the full-length 40-kDa protein. In contrast to the 12-kDa fragment, the untagged C-terminal fragment of EDA was readily recovered by affinity purification on the immobilized receptor and detected by Western blot using anti-EDA antibodies (Fig. 6*A*). N-terminal sequencing of purified processed EDA yielded the sequence SKSNEGADGPVKNKK (Ser^{160}–Lys^{174}), demonstrating that proteolytic cleavage occurred after Arg^{159}. When expressed in 293T cells, mutation R153C did not prevent proteolytic processing of EDA, which still occurred after Arg^{159}. However, partial inhibition of the processing was observed when EDA R153C was expressed in CHO cells (Fig. 6*A*). Mutation R156C, which affects both predicted furin recognition sequences, had a more drastic effect and entirely prevented the degradation of EDA and loss of the FLAG tag in both cell lines (Fig. 6*A*). Interestingly, the unprocessed portion of wt and mutant EDA

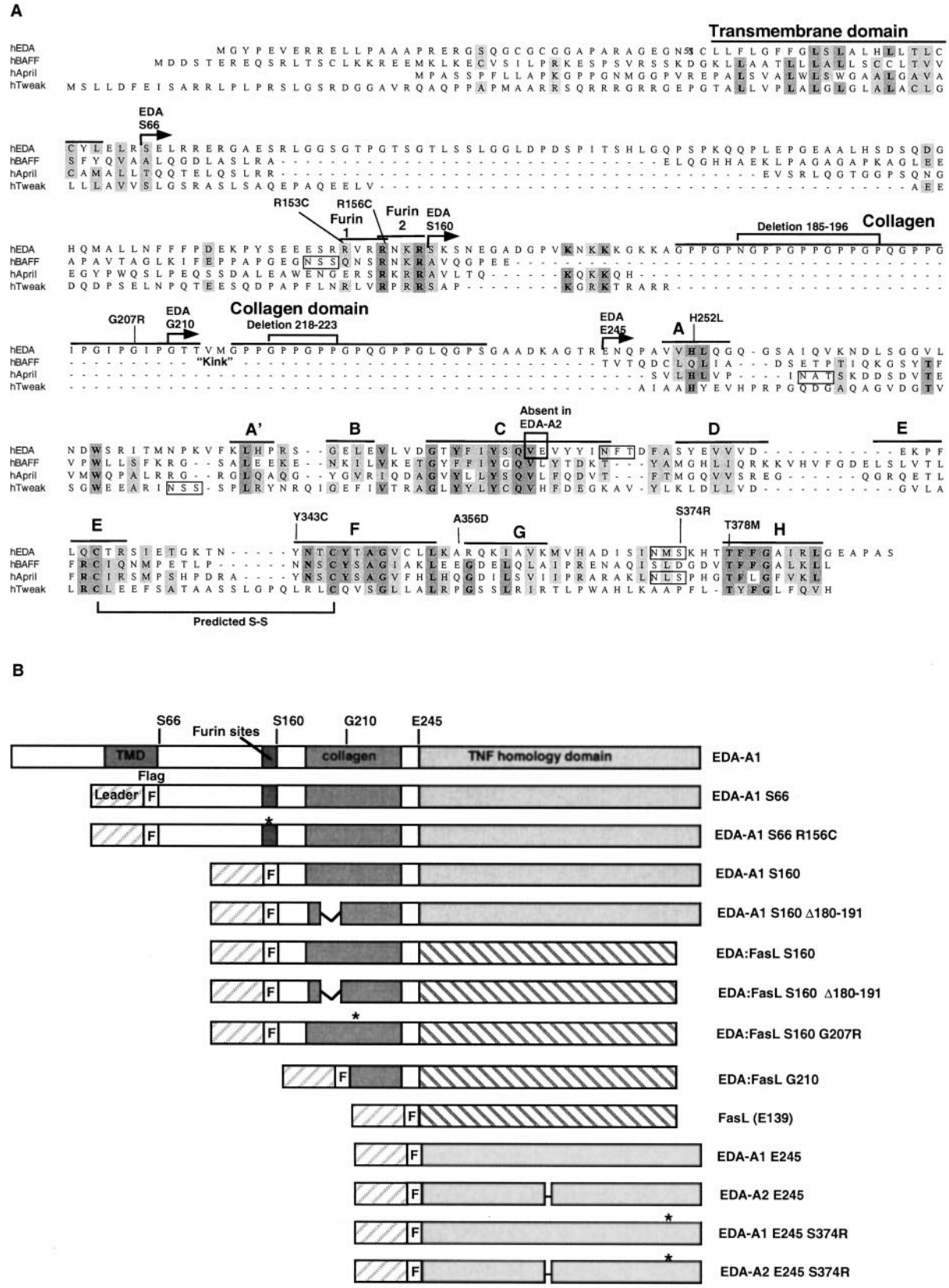

FIG. 1. **Sequence alignment and features of EDA and EDA constructs.** *A,* sequence alignment of EDA and of its closest relatives in the TNF family. The transmembrane domain, furin recognition sequences, collagen domain, and β-sheets A–H of the TNF homology domain are indicated (*bold lines*). The starting position (Ser^{66}, Ser^{160}, Gly^{210}, and Glu^{245}) of the various recombinant proteins is shown by an *arrow*, and the various mutations studied are also indicated. Potential *N*-glycosylation sites are *boxed.* Amino acids Val^{307} and Glu^{308} are absent in EDA-A2, but numbering of mutations in EDA-A1 and EDA-A2 is conserved for clarity. *B,* schematic representation of expression constructs for soluble EDA. *F* = FLAG tag plus a linker of 10 amino acids. Point mutations are indicated by an *asterisk.* In FasL fusion molecules, the TNF homology domain of EDA was replaced by that of FasL.

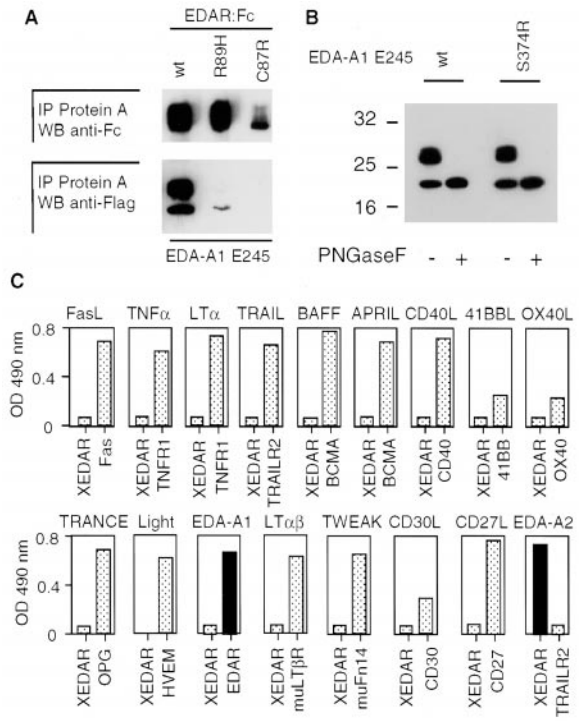

FIG. 2. **Characterization of EDA-A1/EDAR and EDA-A2/XEDAR interactions.** *A,* soluble recombinant EDA-A1 was immunoprecipitated (*IP*) with EDAR:Fc fusion protein (wt or with the indicated mutations) and analyzed by Western blot (*WB*) using anti-FLAG antibody. Precipitated EDAR:Fc is shown in the *top panel. B,* deglycosylation of EDA-A1. EDA-A1s (wt or S374R mutant) were treated ± peptide *N*-glycanase F (*PNGaseF*) and analyzed by Western blot with anti-FLAG antibody. *C,* receptor binding ELISA. XEDAR:Fc, EDAR:Fc, and various control receptors:Fc were captured on an ELISA plate. FLAG-EDA-A1, FLAG-EDA-A2, and various control FLAG ligands were added as indicated. Interactions were revealed using a monoclonal anti-FLAG antibody. Fn14 is a recently described receptor for TWEAK (31).

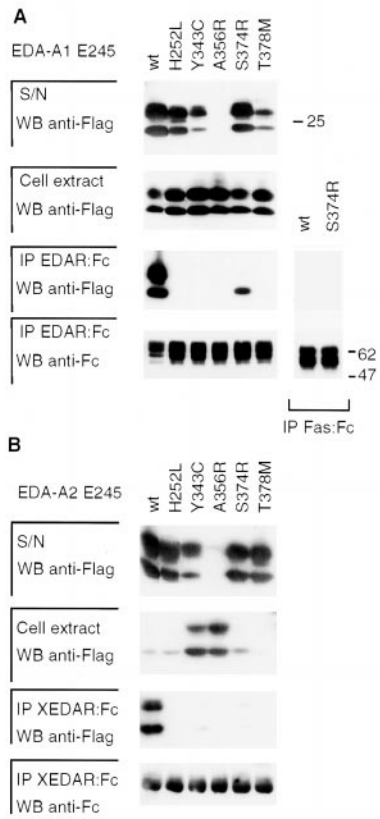

FIG. 3. **Expression and receptor binding of wild type and mutated forms of EDA-A1 and EDA-A2.** *A,* binding of wt and mutant EDA-A1 to EDAR. Supernatants and cell extracts of transfected cells are shown in the *top two panels.* Ligands in supernatants were immunoprecipitated (*IP*) with EDAR:Fc and analyzed by Western blot (*WB*) in the *3rd panel.* Precipitated EDAR:Fc is shown in the *bottom panel.* Results of the immunoprecipitation with a control receptor (Fas:Fc) is shown for EDA-A1 wt and S374R. *B,* binding of wt and mutant EDA-A2 to XEDAR. Analysis was performed essentially as in *B*, except that EDA-A2 and XEDAR were used.

were clearly distinguishable following SDS-polyacrylamide gel electrophoresis under non-reducing conditions, with a proportion of the mutants R153C and R156C migrating as disulfide-linked dimers (Fig. 6*B*). In summary, the results indicate that cleavage of EDA occurs at Arg^{159}, which corresponds to a predicted furin cleavage site, and that mutations within the furin recognition sequence affect the cleavage to various extents.

DISCUSSION

In this study, mutations in the EDA gene were detected in 63% of the families with XLHED, which is lower than the 95% rate we found previously (2) by the direct sequencing of affected males. The lower detection rate is the consequence of two factors. The use of a single set of conditions lowers the sensitivity of SSCP analysis, as only 11 of the 15 known mutations run as controls could be detected under these conditions (73%). In addition, this study included 28% of families with "affected" females only, which was not the case in our previous study. Indeed, the detection rate was lower in families with female probands (45%), and this may well be due to genetic heterogeneity for autosomal forms of HED.

A number of point mutations are located within the TNF homology domain of EDA, but only one of them (Y343C) affects a residue which, based on structural homology with known ligand-receptor structures (4, 5), is predicted to interact with the receptor. Indeed, this mutation abolished receptor binding without affecting the trimeric structure of EDA, although we cannot exclude indirect conformational effects. All other mutations are predicted to have indirect effect on receptor binding, *e.g.* by altering the folding of EDA. It is noteworthy that four independent mutations (G291W, G291R, A356D, R357P) occurred in two short loops at the bottom of EDA (*loops BC* and *FG*, see Fig. 1*A*). The affected amino acids are probably crucial for proper folding of the monomer, as mutation A356D resulted in insoluble EDA-A1 and EDA-A2. Another group of mutations (H252L, S374R) seems to affect the stability of the trimer, because the resulting proteins contain a proportion of monomers. The propensity of unglycosylated subunits to form larger aggregates support the idea that glycosylation of some TNF family members promotes their solubility (18). Interestingly, one of the mutations (S374R) destroys a potential *N*-glycosylation site without affecting the glycosylation of EDA, suggesting that this particular site is not recognized by the *N*-glycosyltransferase. A single mutant (S374R) retained some binding activity to EDAR. Although preferential binding of the unglycosylated (and most probably aggregated) isoform was observed, the interaction appeared specific, suggesting that residual activity may be associated with this mutation *in vivo*. In general, no apparent phenotype/genotype correlation was observed, but the family with missense mutation S374R had two affected males and an affected maternal grandfather with isolated hypodontia. Whether residual activity of this mutant may account for the milder phenotype, and whether there is truly a tissue-specific difference in the function of this mutant protein remains to be determined. Finally, one mutation (T378M) affected secretion and aggregation of EDA-A1 and EDA-A2 in a strikingly different manner. The structural reason for this differential behavior is unclear. In summary, all missense muta-

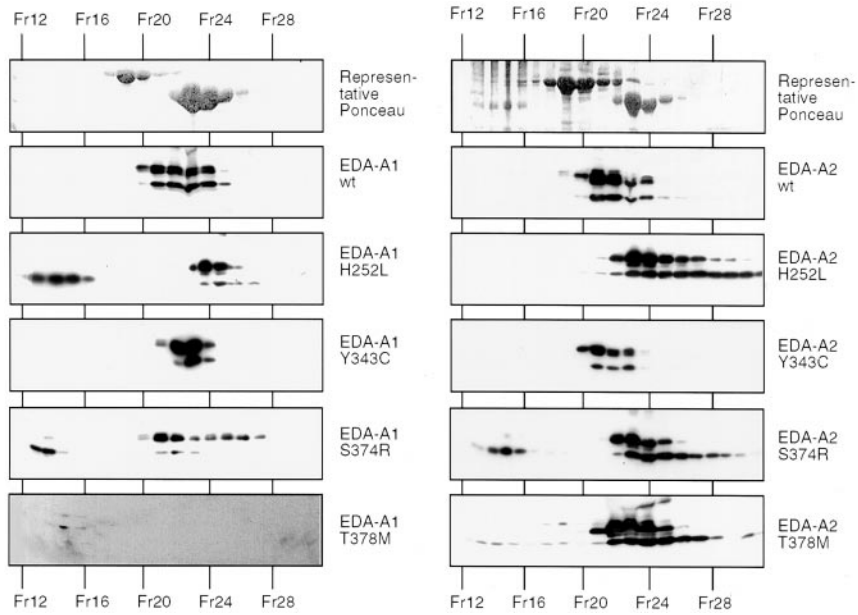

FIG. 4. **Gel filtration analysis of mutated EDA-A1 and EDA-A2.** wt and mutant EDA-A1 Glu^{245} (*left panels*) and EDA-A2 Glu^{245} (*right panels*) were loaded onto a Superdex-200 column and eluted in phosphate-buffered saline. Fractions (700 μl) were precipitated and analyzed by anti-FLAG Western blot. The *top panel* shows Ponceau S staining of the co-injected internal standards catalase and ovalbumin.

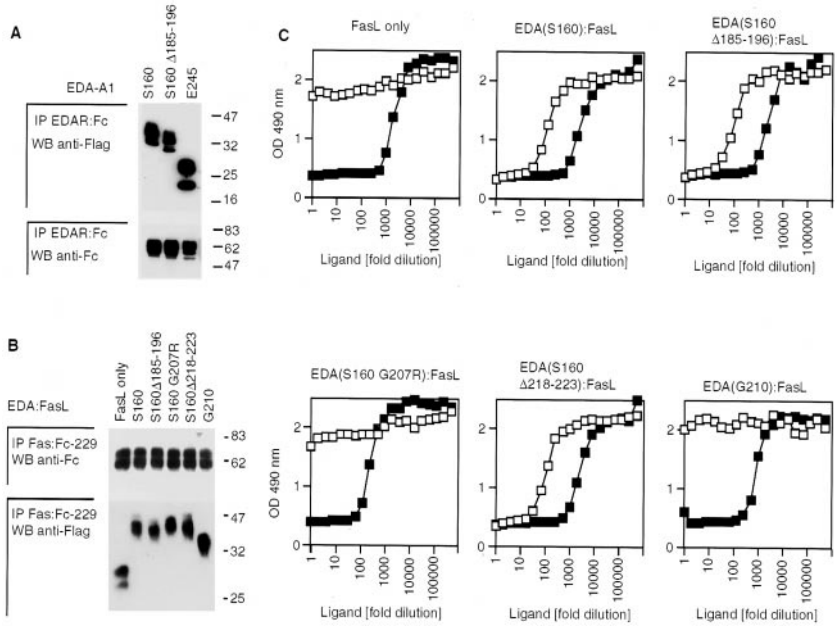

FIG. 5. **Effect of the collagen domain on the receptor activity of EDA-A1 and on the cytotoxic activity of FasL.** *A,* EDA-A1, with or without wild type or mutated collagen domain, was immunoprecipitated (*IP*) with EDAR:Fc and analyzed by Western blot (*WB*) as indicated. *B,* FasL and the various EDA:FasL fusion proteins were immunoprecipitated with Fas:Fc and analyzed by Western blot. *C,* cytotoxic activity of FasL and of the various EDA:FasL fusion proteins was monitored on Jurkat cells, in the presence (*black squares*) or in the absence (*open squares*) of cross-linking anti-FLAG antibody. Cytotoxic activity in the absence of anti-FLAG reveals oligomerization of FasL trimers by the collagen domain of EDA.

tions in the TNF homology domain result in abolished or much impaired binding of EDA-A1 to EDAR and EDA-A2 to XEDAR.

A number of mutations occurring outside the TNF homology domain did not affect binding to the receptor in an *in vitro* assay, indicating that the interaction of EDA with its receptor(s) is necessary but not sufficient for its function *in vivo*. In particular, the integrity of the collagen domain appears to be functionally essential, and we provided evidence that it may serve to multimerize EDA trimers. This is in strong support of the hypothesis that EDA belongs to the C1q as well as to the TNF family of proteins (19). C1q family members are characterized by the presence of a C-terminal globular trimeric domain, with striking structural homology to TNF (20), which is prolonged by a collagen triple helix further assembling into an N-terminal bundle structure, giving rise to a highly multimeric superstructure. In the TNF family, it has been shown that the activity of soluble trimers can be dramatically increased by antibody-mediated multimerization, thereby mimicking the membrane-bound form of the ligand (16, 21). A highly multimeric structure of EDA would provide a powerful means for the soluble protein to signal through high valency receptor clustering. In line with this hypothesis, we found that a naturally occurring point mutation (G207R) in the collagen domain completely abolished the bundle effect. It is, however, likely that the collagen domain also serves additional functions; a number of families with XLHED displayed in frame deletion of 2 or 4 Gly*XY* repeats in the predicted bundle domain of the collagen triple helix, *i.e.* before the interruption in the Gly*XY* repeats. Deletions of 2 Gly*XY* repeats can also be found C-terminal to the interruption. Surprisingly, the activity of recombinant proteins containing these types of deletions was indistinguishable from wild type, at least in the model systems utilized. The deletions may specifically affect multimerization of the collagen domain under *in vivo* conditions. Alternatively, the collagen domain may have additional functions, *e.g.* interaction with other proteins. It is well known for C1q that the collagen domain interacts with the serine proteases C1r and C1s to form C1, the first component of the serum complement system, and with a number of other proteins, including membrane-bound receptors (22). Further investigations are required to under-

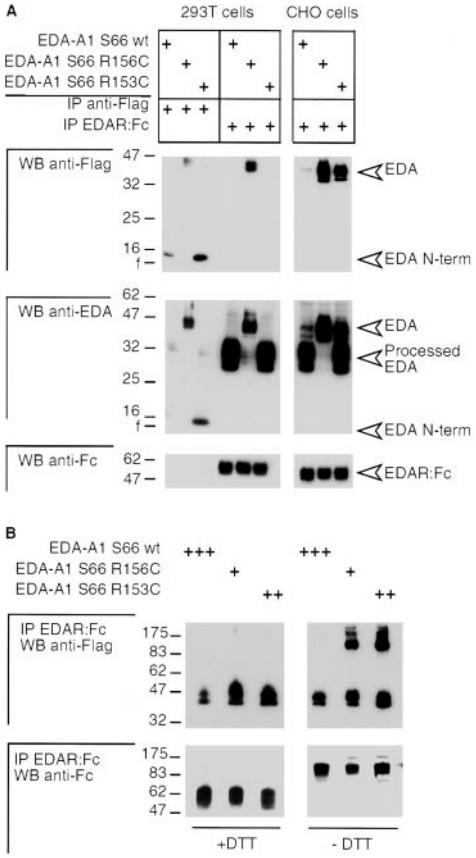

FIG. 6. **Effect of mutations in the furin recognition sequence of EDA-A1.** *A,* the indicated EDA-A1 constructs were transfected in both 293T and CHO cells, and cell supernatants were collected and immunoprecipitated (*IP*) with anti-FLAG antibody or with EDAR:Fc. Immunoprecipitates were analyzed by Western blot (*WB*) using either anti-FLAG or anti-EDA antibodies. The identity of the observed fragments is indicated on the *right-hand side.* Proteolytic processing results in loss of the FLAG tag, which is recovered as a small N-terminal fragment (*EDA N-term*). *B,* supernatants of CHO cells transfected with the indicated EDA-A1 constructs were immunoprecipitated with EDAR:Fc, treated plus or minus dithiothreitol (*DTT*), and analyzed by Western blot with anti-FLAG antibodies. Different volumes of supernatants (indicated by +, ++, and +++) were utilized to compensate for the loss of FLAG tag after furin-mediated processing.

stand the molecular mechanism underlying loss of function of EDA in these particular deletion mutants.

15 families with XLHED displayed 5 distinct mutations in the furin consensus recognition sequences of EDA, demonstrating an important functional role for this 7-aa sequence. The release of soluble EDA upon proteolytic processing is an expected event, as mRNAs for EDA and EDAR are not expressed in adjacent cells but rather in spatially distinct tissues, at least in the developing tooth (10). EDA contains two overlapping furin recognition sequences (RVRR and RNKR spanning aa 153–156 and 156–159, respectively). Because Arg^{156} is part of both sequences, it is hardly surprising that mutation R156C completely abolished EDA processing. Mutation R153C also affected the cleavage of EDA, but in a less dramatic manner. Although this mutation destroys only one of the two furin sites, this must be sufficiently disturbing to prevent efficient release of EDA from the cells naturally expressing it. These cells may express low amounts of furin or furin isoforms whose specificity may extend further than the canonical tetrapeptide recognition sequence. However, as mutations affecting the first furin domain invariably yield Cys residues, and as these Cys residues appear to form novel disulfide bridges, it is possible that this novel structural constraint prevents proper recognition of the remaining intact furin site. It also clearly appears from this study that, beside the furin cleavage sites, there are no alternative sites for solubilization of EDA. In particular, the sequence RRER (aa 69–72) and the basic motives KNKK and KGKK (aa 171–174 and 175–178) were not cleaved in our expression system. The latter two motifs are encoded in the small exon 4 and are also found in the sequences of Tweak and APRIL. However, mutations in these sequences have not been described so far in association with XLHED.

A single splice site mutation was detected in the current study (IVS8 $G^{+5} \rightarrow A$), which affects the splice donor site of exon 8 utilized to generate the 391-aa EDA-A1 isoform of the ligand. EDA-A2 utilizes an alternate splice site 6 base pairs 5′ to this site. This mutation probably interferes with splicing of EDA-A1 but not EDA-A2, as computer analysis by HSPL (prediction of splice sites in human DNA sequence) demonstrates a complete loss of the A1 but not of the A2 donor site. This together with the fact that genetic defects in EDA and in EDAR both lead to identical phenotypes indicate a crucial role for EDA-A1/EDAR interactions during morphogenesis. The role of the parallel EDA-A2/XEDAR interaction is less well established. If at all involved in hair, sweat gland, and teeth formation, it is not able to rescue a genetic deficiency in EDAR. In addition, there is no evidence to date for mutations in XEDAR being associated with the HED phenotype. XEDAR may play a distinct role in skin development, which does not translate into an HED phenotype upon dysfunction. Alternatively, inactivation of XEDAR might be lethal, but this would only be possible if it binds another ligand beside EDA-A2 or fulfills a vital, ligand-independent function. TROY/TAJ is a close sequence homologue of XEDAR, which is also expressed in the developing skin (23, 24). The precise functional roles of XEDAR and TROY and their interplay with the EDAR pathway remain to be determined.

Acknowledgments—We thank the families who participated in these studies and the many clinicians who provided both samples and clinical information. We thank Dr. Teresa Cachero, Dr. Jeffrey Browning, and Dr. Matvey Lukashev (Biogen Inc., Cambridge, MA) for their help with protein sequencing and for the identification of the XEDAR cDNA clone. We are grateful to Dr. Steven R. Wiley (Immunex Corp., Seattle, WA) for the authorization to show the Fn14-TWEAK interaction prior to publication.

REFERENCES

1. Bayes, M., Hartung, A. J., Ezer, S., Pispa, J., Thesleff, I., Srivastava, A. K., and Kere, J. (1998) *Hum. Mol. Genet.* **7,** 1661–1669
2. Monreal, A. W., Zonana, J., and Ferguson, B. (1998) *Am. J. Hum. Genet.* **63,** 380–389
3. Yan, M., Wang, L. C., Hymowitz, S. G., Schilbach, S., Lee, J., Goddard, A., de Vos, A. M., Gao, W. Q., and Dixit, V. M. (2000) *Science* **290,** 523–527
4. Hymowitz, S. G., O'Connell, M. P., Ultsch, M. H., Hurst, A., Totpal, K., Ashkenazi, A., de Vos, A. M., and Kelley, R. F. (2000) *Biochemistry* **39,** 633–640
5. Banner, D. W., D'Arcy, A., Janes, W., Gentz, R., Schoenfeld, H. J., Broger, C., Loetscher, H., and Lesslauer, W. (1993) *Cell* **73,** 431–445
6. Moore, P. A., Belvedere, O., Orr, A., Pieri, K., LaFleur, D. W., Feng, P., Soppet, D., Charters, M., Gentz, R., Parmelee, D., Li, Y., Galperina, O., Giri, J., Roschke, V., Nardelli, B., Carrell, J., Sosnovtseva, S., Greenfield, W., Ruben, S. M., Olsen, H. S., Fikes, J., and Hilbert, D. M. (1999) *Science* **285,** 260–263
7. Schneider, P., MacKay, F., Steiner, V., Hofmann, K., Bodmer, J. L., Holler, N., Ambrose, C., Lawton, P., Bixler, S., Acha-Orbea, H., Valmori, D., Romero, P., Werner-Favre, C., Zubler, R. H., Browning, J. L., and Tschopp, J. (1999) *J. Exp. Med.* **189,** 1747–1756
8. Hahne, M., Kataoka, T., Schroter, M., Hofmann, K., Irmler, M., Bodmer, J. L., Schneider, P., Bornand, T., Holler, N., French, L. E., Sordat, B., Rimoldi, D., and Tschopp, J. (1998) *J. Exp. Med.* **188,** 1185–1190
9. Chicheportiche, Y., Bourdon, P. R., Xu, H., Hsu, Y. M., Scott, H., Hession, C., Garcia, I., and Browning, J. L. (1997) *J. Biol. Chem.* **272,** 32401–32410
10. Tucker, A. S., Headon, D. J., Schneider, P., Ferguson, B. M., Overbeek, P., Tschopp, J., and Sharpe, P. T. (2000) *Development* **127,** 4691–4700
11. Headon, D. J., and Overbeek, P. A. (1999) *Nat. Genet.* **22,** 370–374
12. Monreal, A. W., Ferguson, B. M., Headon, D. J., Street, S. L., Overbeek, P. A., and Zonana, J. (1999) *Nat. Genet.* **22,** 366–369
13. Zonana, J., Elder, M. E., Schneider, L. C., Orlow, S. J., Moss, C., Golabi, M., Shapira, S. K., Farndon, P. A., Wara, D. W., Emmal, S. A., and Ferguson, B. M. (2000) *Am. J. Hum. Genet.* **67,** 1555–1562

14. Ferguson, B. M., Thomas, N. S., Munoz, F., Morgan, D., Clarke, A., and Zonana, J. (1998) *J. Med. Genet.* **35,** 112–115
15. Schneider, P. (2000) *Methods Enzymol.* **322,** 325–345
16. Schneider, P., Holler, N., Bodmer, J. L., Hahne, M., Frei, K., Fontana, A., and Tschopp, J. (1998) *J. Exp. Med.* **187,** 1205–1213
17. Kishore, U., and Reid, K. B. (1999) *Immunopharmacology* **42,** 15–21
18. Schneider, P., Bodmer, J. L., Holler, N., Mattmann, C., Scuderi, P., Terskikh, A., Peitsch, M. C., and Tschopp, J. (1997) *J. Biol. Chem.* **272,** 18827–18833
19. Mikkola, M. L., Pispa, J., Pekkanen, M., Paulin, L., Nieminen, P., Kere, J., and Thesleff, I. (1999) *Mech. Dev.* **88,** 133–146
20. Shapiro, L., and Scherer, P. E. (1998) *Curr. Biol.* **8,** 335–338
21. Grell, M., Douni, E., Wajant, H., Lohden, M., Clauss, M., Maxeiner, B., Georgopoulos, S., Lesslauer, W., Kollias, G., and Pfizenmaier, K. (1995) *Cell* **83,** 793–802
22. Eggleton, P., Reid, K. B., and Tenner, A. J. (1998) *Trends Cell Biol.* **8,** 428–431
23. Kojima, T., Morikawa, Y., Copeland, N. G., Gilbert, D. J., Jenkins, N. A., Senba, E., and Kitamura, T. (2000) *J. Biol. Chem.* **275,** 20742–20747
24. Eby, M. T., Jasmin, A., Kumar, A., Sharma, K., and Chaudhary, P. M. (2000) *J. Biol. Chem.* **275,** 15336–15342
25. Kere, J., Srivastava, A. K., Montonen, O., Zonana, J., Thomas, N., Ferguson, B., Munoz, F., Morgan, D., Clarke, A., Baybayan, P., Chen, E. Y., Ezer, S., Saarialho-Kere, U., de la Chapelle, A., and Schlessinger, D. (1996) *Nat. Genet.* **13,** 409–416
26. Hertz, J. M., Norgaard Hansen, K., Juncker, I., Kjeldsen, M., and Gregersen, N. (1998) *Clin. Genet.* **53,** 205–209
27. Martinez, F., Millan, J. M., Orellana, C., and Prieto, F. (1999) *J. Invest. Dermatol.* **113,** 285–286
28. Yotsumoto, S., Fukumaru, S., Matsushita, S., Oku, T., Kobayashi, K., Saheki, T., and Kanzaki, T. (1998) *J. Invest. Dermatol.* **111,** 1246–1247
29. Aoki, N., Ito, K., Tachibana, T., and Ito, M. (2000) *J. Invest. Dermatol.* **115,** 329–330
30. Orth, U., and Gal, A. (1998) *Am. J. Hum. Genet.* **63,** 377
31. Cassiano, L., Smith, C. A., Goodwin, R. G., and Wiley, S. R. (2000) *Scand. J. Immunol.* **51,** Suppl. 1, 22